Title:

Mutation-specific downregulation of CFTR2 variants by gating potentiators

Authors:

Radu G. Avramescu, Yukari Kai, Haijin Xu, Aurélien Bidaud-Meynard, Andrea Schnúr, Saul Frenkiel, Elias Matouk, Guido Veit, Gergely L. Lukacs

Online Data Supplement

Supplementary figures

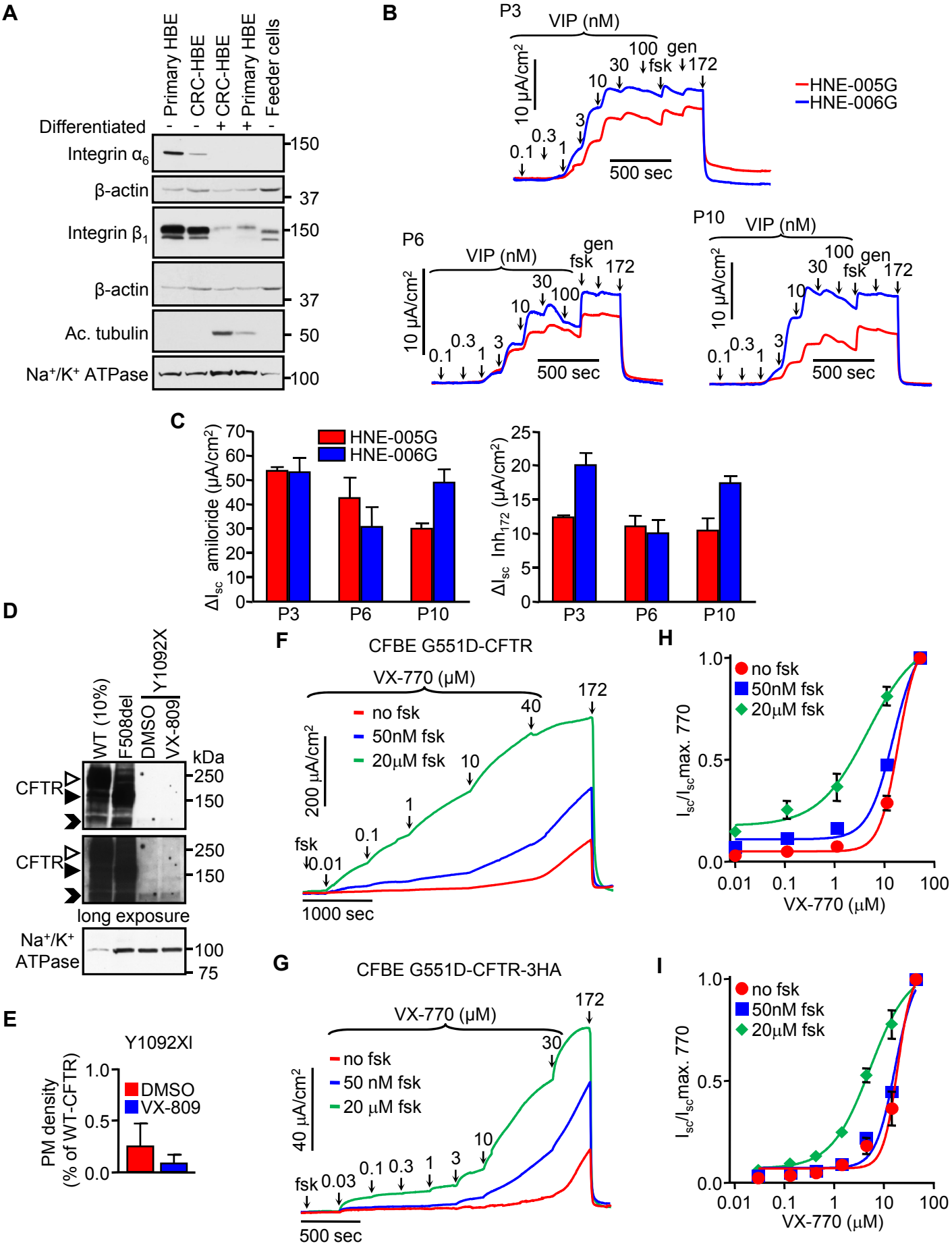

Figure E1. The electrophysiological phenotype of HNE is stable over multiple passages. **(A)** Primary HBE are reprogrammed and expanded in medium F in presence of irradiated 3T3-J2 feeder cells and ROCK inhibitor (Y-27632, 10 μM) followed by differentiation in Ultroser G medium on Snapwell filter membrane supports under air-liquid (ALI) conditions. Immunoblot shows down-regulation of cell-matrix adhesion molecules integrin β_1 and α_6 and up-regulation of cilium marker acetylated tubulin upon differentiation and polarization in Ultroser G medium under ALI for 4 weeks as indicated. Non-polarized HBE cells were cultured on collagen coated dishes until passage 2. **(B)** CR-HNE from two *CFTR*$^{WT/WT}$ donors (donor code: HNE-005G and HNE-006G) were propagated for 10 passages and their electrophysiological properties were compared after differentiation for passages (P) 3, 6 and 10 by I_{sc} measurement. **(C)** Comparison between cells differentiated at passages 3, 6, 10 showed similar amiloride-sensitive (100 μM) ENaC currents and $CFTR_{Inh}$-172 sensitive (172, 20 μM) CFTR currents after stimulation with vasoactive intestinal peptide (VIP), forskolin (fsk, 20 μM) and genistein (gen, 50 μM). Experiments performed in presence of a basolateral-to-apical chloride gradient; error bars are SD of three parallel measurements. **(D)** Immunoblots of CFBE cells expressing the indicated CFTR constructs after incubation for 24h with and without VX-809 (3 μM). CFTR was detected with anti-HA antibody, Na^+/K^+ ATPase served as loading control. The empty arrowheads show the mature, complex glycosylated CFTR protein (C-band), the filled arrowhead show the immature, core glycosylated protein (B-band) and the filled chevrons show truncated core glycosylated protein. **(E)** PM density of CFBE cells expressing Y1092X-CFTR mutant after 24h treatment with and without VX-809 (3 μM). The PM densities were normalized for cell viability and are expressed as % of WT-CFTR. **(F, G)** I_{sc} of CFBE cells expressing CFTR-G551D (D) or CFTR-G551D with an extracellular 3HA tag (E) under the control of a TetON doxycycline controlled transactivator. CFTR was activated with the indicated forskolin (fsk) concentrations followed by VX-770 titration. The specificity of the short circuit current was verified by adding the CFTR-specific inhibitor, $CFTR_{inh}$-172 (20 μM). Measurements were performed in the presence of a basolateral-to-apical chloride gradient after basolateral permeabilization with amphotericin B (100 μM). **(H, I)** Dose-response to VX-770 stimulation of G551D-CFTR (F) or CFTR-G551D with an extracellular 3HA tag (G) without stimulated phosphorylation (no fsk, non-tagged EC_{50} = 19.17 ±1.24 μM, 3HA-tagged EC_{50} = 20.10 ±1.67 μM), low phosphorylation (50 nM fsk, non-tagged EC_{50} = 15.05 ±1.01 μM, 3HA-tagged EC_{50} = 18.27 ±1.13 μM) and high phosphorylation (20 μM fsk, non-tagged EC_{50} = 4.62 ±1.36 μM, 3HA-tagged EC_{50} = 5.57 ±0.48 μM). Measurements were performed in the presence of a basolateral-to-apical chloride gradient after basolateral permeabilization with amphotericin B (100 μM). All CFBE experiments are n=3, error bars are SEM.

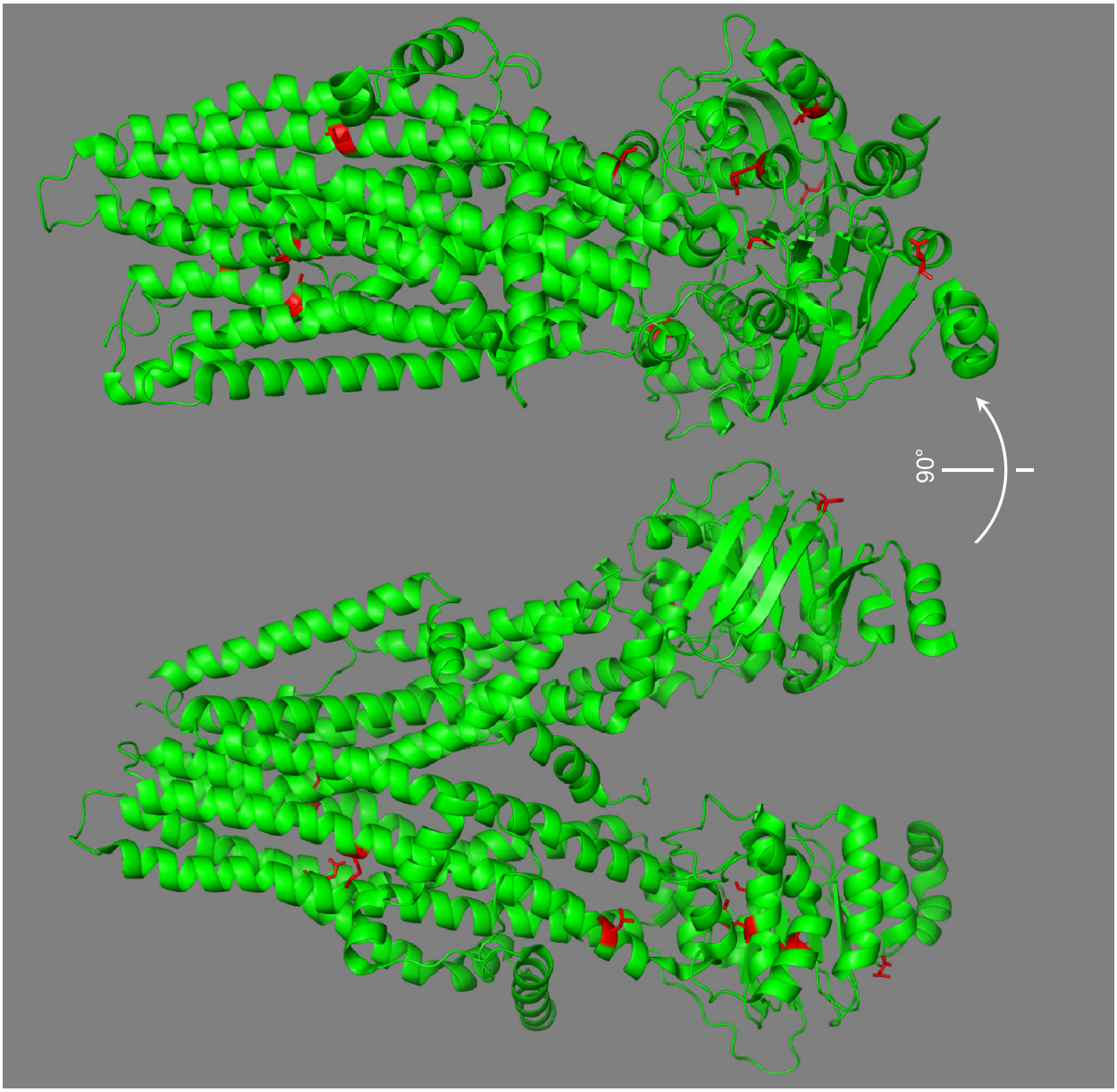

Figure E2. Selected CFTR2 mutations are distributed throughout the four major domains of CFTR. **(A)** High resolution electron cryo-microscopy model (1) of human CFTR showing the positions of the selected CFTR2 mutations in red. 90° rotation of the molecule is given, for better exposition of mutation position. The structure reiterates Fig. 2A.

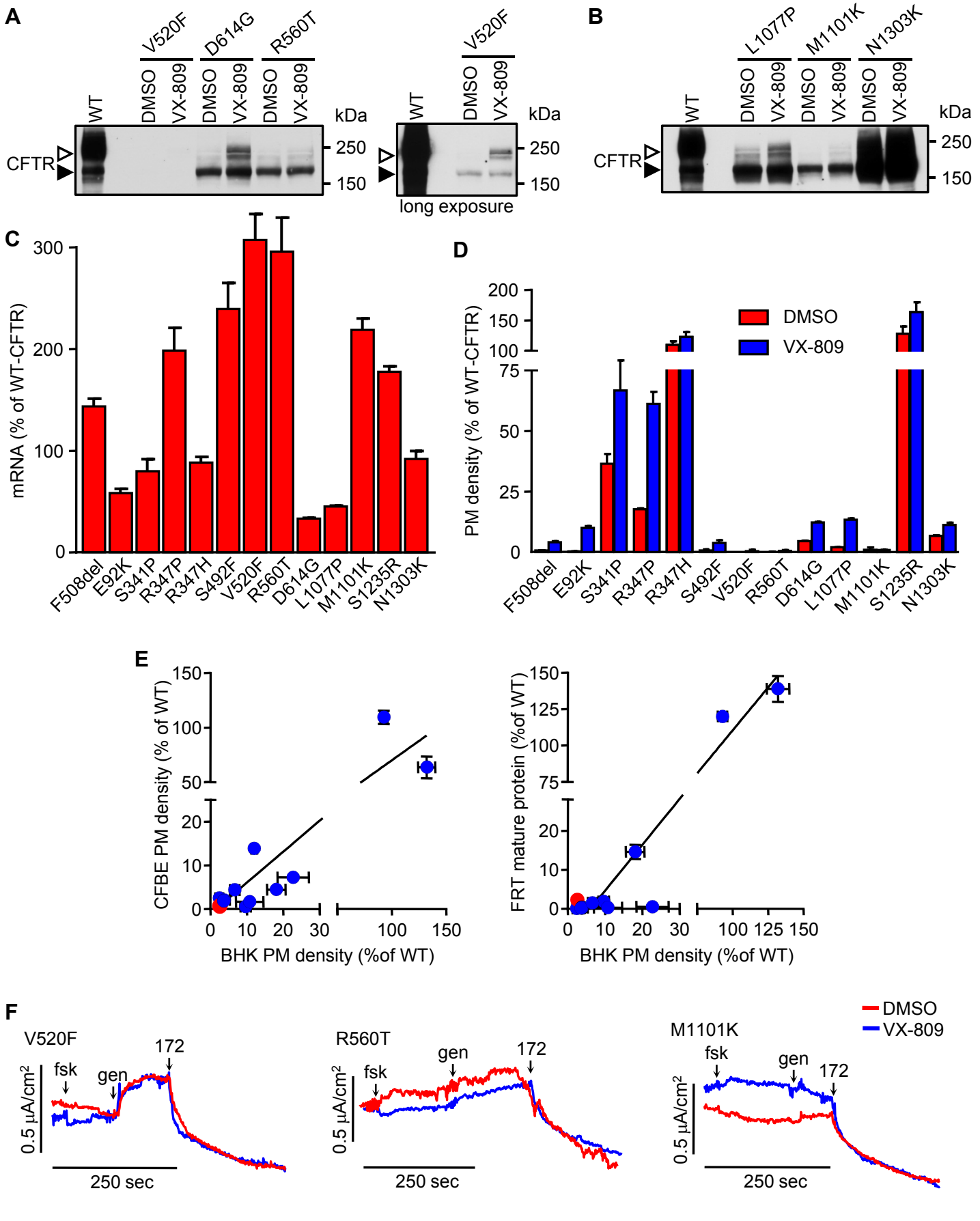
A
WT
V520F
D614G
R560T
DMSO
VX-809
CFTR
kDa
250
150
long exposure
B
L1077P
M1101K
N1303K
C
mRNA (% of WT-CFTR)
F508del
E92K
S341P
R347P
R347H
S492F
V520F
R560T
D614G
L1077P
M1101K
S1235R
N1303K
D
PM density (% of WT-CFTR)
E
CFBE PM density (% of WT)
BHK PM density (%of WT)
FRT mature protein (%of WT)
F
V520F
R560T
M1101K
fsk
gen
172
0.5 µA/cm²
250 sec

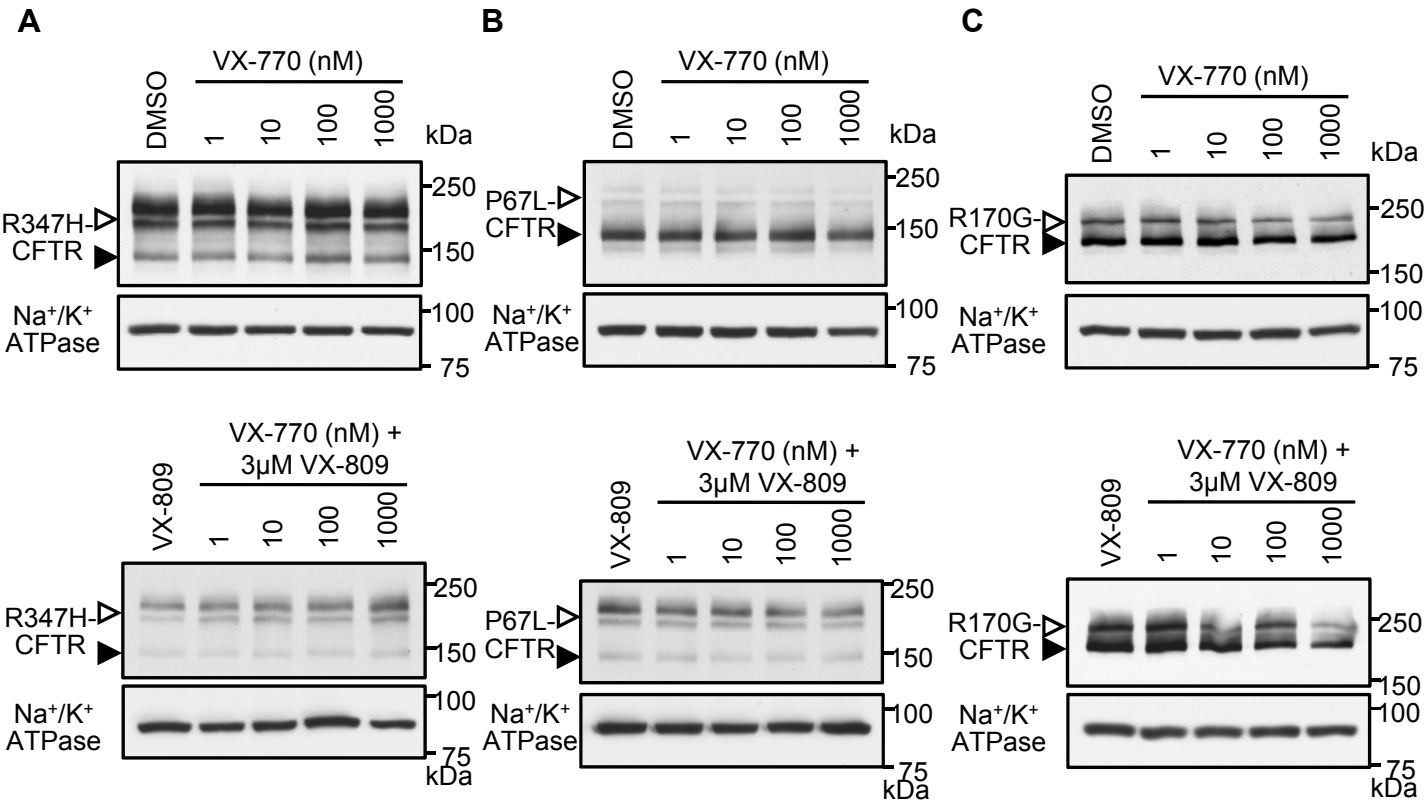

Figure E4. (A-C) CFBE cells expressing the indicated CFTR mutants were incubated for 24h increasing concentrations of VX-770 (*top*) with and without VX-809 (3 μM, *bottom*) and subsequently lysed to collect protein samples. Protein was detected by immunoblotting with anti-HA antibody. Na^+/K^+ ATPase was used as loading control. The empty arrowheads show the mature, complex glycosylated CFTR protein (C-band), and the filled arrowhead show the immature, core glycosylated protein (B-band).

Supplementary tables

Table E1. CFTR mutation list.

cDNA Name	Protein Name	Legacy Name
c.200C>T	p.Pro67Leu	P67L
c.274G>A	p.Glu92Lys	E92K
c.508C>G	p.Arg170Gly	R170G
c.1021T>C	p.Ser341Pro	S341P
c.1040G>C	p.Arg347Pro	R347P
c.1040G>A	p.Arg347His	R347H
c.1475C>T	p.Ser492Phe	S492F
c.1521_1523delCTT	p.Phe508del	F508del
c.1558G>T	p.Val520Phe	V520F
c.1652G>A	p.Gly551Asp	G551D
c.1679G>C	p.Arg560Thr	R560T
c.1841A>G	p.Asp614Gly	D614G
c.3230T>C	p.Leu1077Pro	L1077P
c.3276C>A or c.3276C>G	p.Tyr1092X	Y1092X
c.3302T>A	p.Met1101Lys	M1101K
c.3705T>G	p.Ser1235Arg	S1235R
c.3909C>G	p.Asn1303Lys	N1303K

List of CFTR (RefSeq NM_000492.3) mutants used throughout the entirety of this work.

Table E2. Pearson correlation coefficient matrix.

Mutant		E92K	L1077P	S1235R	S1235R
	VX-809	-	-	-	+
E92K	-				
L1077P	-	0.450			
S1235R	-	0.454	0.334		
S1235R	+	0.444	0.285	0.938	

Pearson correlation coefficient matrix calculated for the indicated CFTR mutants with respect to the effect of the twelve potentiators used for long term treatment on PM density.

Table E3. p-value matrix.

Mutant		E92K	L1077P	S1235R	S1235R
	VX-809	-	-	-	+
E92K	-				
L1077P	-	0.141339			
S1235R	-	0.137338	0.288212		
S1235R	+	0.147773	0.368014	6.16E-06	

Associated p-values calculated for the Pearson coefficients in Table E1.

Supplementary methods

Primary nasal epithelium collection, conditional reprogramming and differentiation

A complete protocol for the isolation of human nasal epithelia has been published (2). Briefly, primary nasal scrapes are harvested from the upper nasal turbinates of a donor under otoscopic observation and are quickly deposited in RPMI 1640 medium kept on ice. Explants are detached from the curettes and are seeded on collagen VII coated plastic 12 well plates with a minimum volume of BEGM. The epithelial cells are expected to migrate out of the explants overnight and are subsequently grown to confluence. To conditionally reprogram the HNE, cells are cocultured with irradiated 3T3-J2 fibroblasts (non-dividing), which act as feeder cells, in the presence of Rho-associated protein kinase (ROCK) inhibitor Y-27632 (10μM) (3). Under these conditions, the primary nasal epithelial cells can be expanded without undergoing senescence or terminal differentiation.

Primary bronchial and nasal cell differentiation

Epithelial cell differentiation has been previously described (4). In brief, to obtain a polarized epithelial monolayer, bronchial or nasal cells are seeded onto Snapwell filter inserts at a confluence of $0.5x10^6$ cells/filter. The monolayers are then differentiated under air-liquid interface by culturing in Ultroser G (Pall Corporation, Saint-Germain-en-Laye, France) medium for a minimum of four weeks (4).

Short-circuit current measurement

Current measurements were performed for CFBE, HBE and HNE cells as previously described (5, 6). Briefly, CFBE cells, expressing a channel variant or conditionally

reprogrammed primary airway cells are grown on filter insets in order to induce polarized expression of CFTR (RefSeq NM_000492.3). Once mounted in the Ussing assembly, the apical side is immersed in an isotonic, low chloride solution, while the basolateral side is immersed in Krebs-Ringer bicarbonate solution.

CFTR PM Density Measurements by Luminescence and Fluorescence Assays

In a 96-well format, the CFTR PM density was assessed by a modified enzyme-linked immunosorbent assay (ELISA) protocol (5). After the addition of chemiluminescent substrate (SuperSignal West Pico, Thermo Fisher Scientific), the luminescence signal was measured in a VICTOR Light plate reader (PerkinElmer).

If the signal was low, the ELISA signal was determined using Amplex Red (Thermo Fisher Scientific) as HRP substrate, in a 24 well format, as described (7). After addition of the fluorogenic substrate, cells were incubated for 5-15 minutes at room temperature. The fluorescence signal was measured with Infinite M1000 fluorescence plate reader (TECAN). For both types of density measurement, the signal was normalized with cell viability determined by alamarBlue (Thermo Fisher Scientific) assay, as described (8).

Immunofluorescence

CR-HNE and CR-HBE were differentiated for a minimum of 4 weeks in UltroserG medium at ALI. Filters were washed twice for 2 min at 37°C with PBS followed by 2 rapid PBS washes to remove mucins. Cells were then fixed (4% PFA, 10 min), permeabilized (0.2% Triton X-100, 5 min) and blocked (0.5% BSA in PBS + 0.1 mM Ca^{2+} + 1mM Mg^{2+}, 1 h), then incubated overnight at 4°C with primary antibodies against acetylated tubulin (1:200, sigma

T7451), zonula occludens-1 (1:100, Invitrogen 402200) or mucin5AC (1:200, Thermo Scientific 45M MS145PO). Nuclei were stained with DAPI (1:5000, Sigma D9542). After washing (4 times, 5 min with PBS), the cells were incubated with the following secondary antibodies at room temperature: mouse-A488 (1:1500, 1 h); rabbit-A555 (1:1000, 1 h). After washing (4 times, 5 min with PBS), the filter inserts were mounted between a glass slide and a coverslip and images were acquired with a Zeiss LSM 780 confocal microscope (Carl Zeiss Canada, Toronto, Ontario, Canada) equipped with a Plan-Apochromat 63x/1.40 oil differential interference contrast objective.

Quantitative RT-PCR

Total RNA was extracted from polarized CFBE cells grown on plastic in 24 well plates using miRNeasy Mini Kit (Qiagen, Hilden, Germany) and analyzed using the one-step QuantiFast SYBR Green RT-PCR Kit (Qiagen) following the manufacturer's recommendations. Data were analyzed by efficiency-corrected comparative quantification with MxPro QPCR software (Agilent, Santa Clara, California, USA). CFTR was detected with primers sense gaggaaaggatacagacagcgcctg and antisense gaagccagctctctatcccattc. Variations in RNA loading amount were accounted for by normalizing to GAPDH (sense primer catgagaagtatgacaacagcct, antisense primer agtccttccacgataccaaagt).

Supplementary References

1. Van Goor F, Yu H, Burton B, Hoffman BJ. Effect of ivacaftor on CFTR forms with missense mutations associated with defects in protein processing or function. J Cyst Fibros. 2014;13(1):29-36.

2. Muller L, Brighton LE, Carson JL, Fischer WA, 2nd, Jaspers I. Culturing of human nasal epithelial cells at the air liquid interface. Journal of visualized experiments : JoVE. 2013(80):e50646.

3. Liu X, Ory V, Chapman S, Yuan H, Albanese C, Kallakury B, et al. ROCK inhibitor and feeder cells induce the conditional reprogramming of epithelial cells. The American journal of pathology. 2012;180(2):599-607.

4. Neuberger T, Burton B, Clark H, Van Goor F. Use of primary cultures of human bronchial epithelial cells isolated from cystic fibrosis patients for the pre-clinical testing of CFTR modulators. Methods in Molecular Biology (Clifton, Nj). 2011;741:39-54.

5. Veit G, Bossard F, Goepp J, Verkman AS, Galietta LJ, Hanrahan JW, et al. Proinflammatory Cytokine Secretion is Suppressed by TMEM16A or CFTR Channel Activity in Human Cystic Fibrosis Bronchial Epithelia. Molecular biology of the cell. 2012.

6. Namkung W, Finkbeiner WE, Verkman AS. CFTR-adenylyl cyclase I association responsible for UTP activation of CFTR in well-differentiated primary human bronchial cell cultures. Molecular biology of the cell. 2010;21(15):2639-48.

7. Glozman R, Okiyoneda T, Mulvihill CM, Rini JM, Barriere H, Lukacs GL. N-glycans are direct determinants of CFTR folding and stability in secretory and endocytic membrane traffic. J Cell Biol. 2009;184(6):847-62.

8. Veit G, Avramescu RG, Perdomo D, Phuan PW, Bagdany M, Apaja PM, et al. Some gating potentiators, including VX-770, diminish ΔF508-CFTR functional expression. Sci Transl Med. 2014;6(246):246ra97.